

Plasmoid-mediated reconnection during nonlinear relaxation of peeling-ballooning edge-localized modes

Fatima Ebrahimi

NSTX-U research meeting

January 10, 2022

PPPL

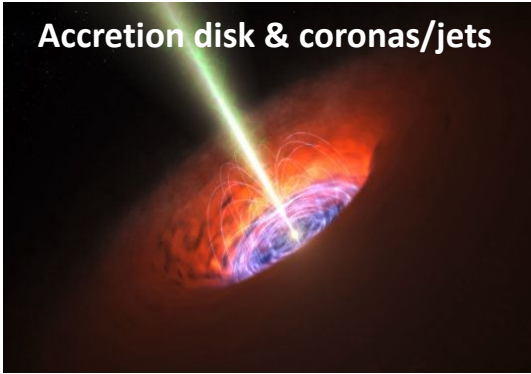
F. Ebrahimi, Plasmoid-mediated reconnection during Peeling-Ballooning ELMs (under review)

<https://arxiv.org/abs/2110.09706>

Thanks: A. Bhattacharjee, G. Dong, Z. Lin and D. Brennan

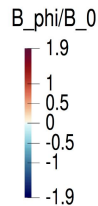
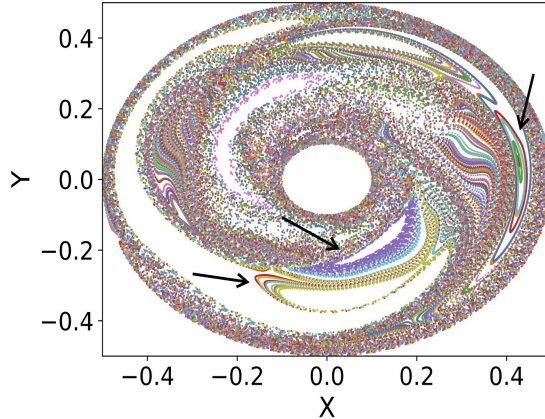


Accretion disk & coronas/jets



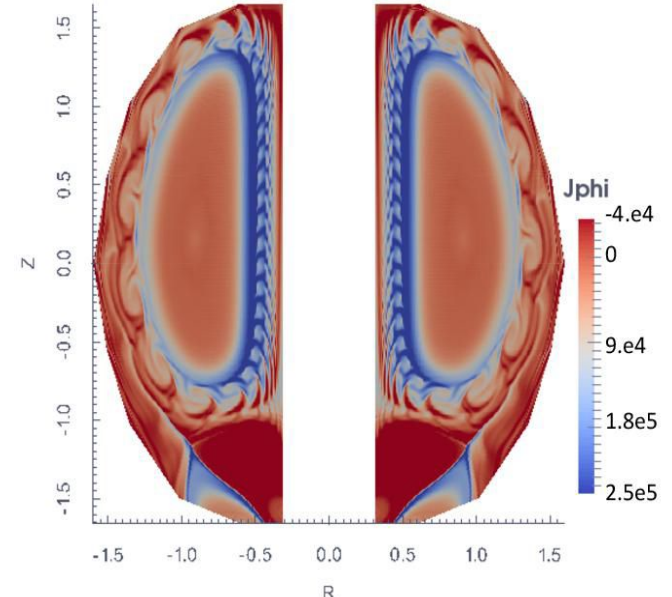
I -In astrophysical disks Magnetic islands in accretion flows

Toroidal Cross Section

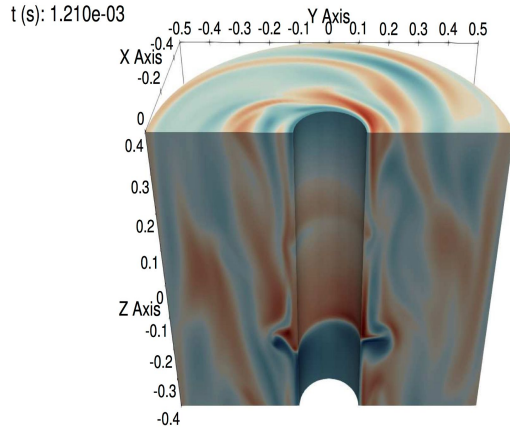


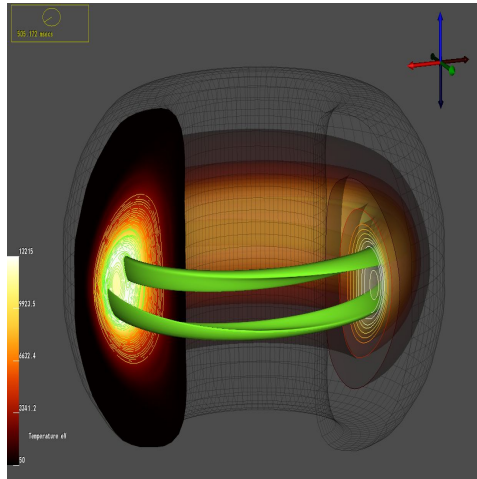
Rosenberg & Ebrahimi
ApJL 2021

II- In a tokamak ELM nonlinear dynamics

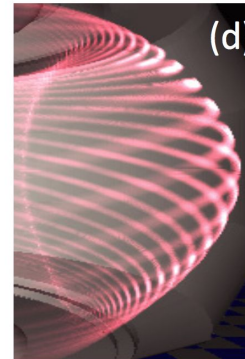
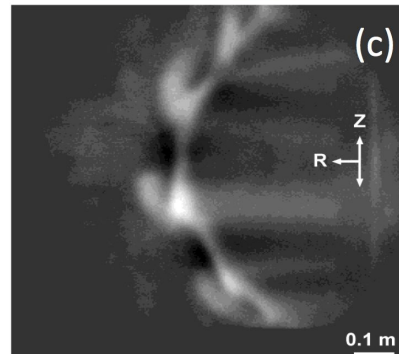
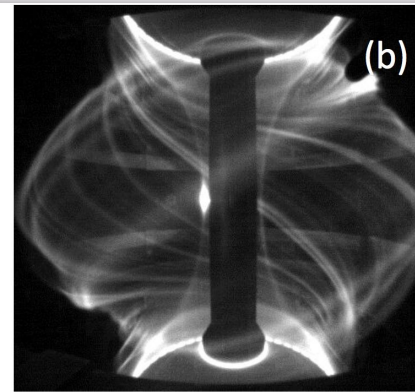
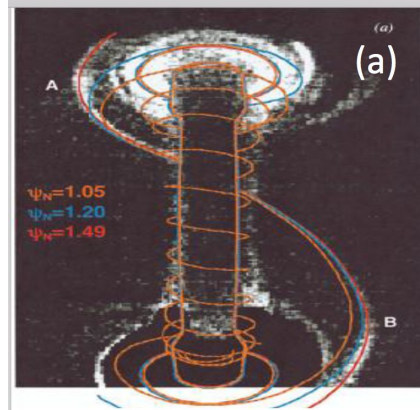


Onset and relaxation of SOL
currents.
Ebrahimi PoP 2017



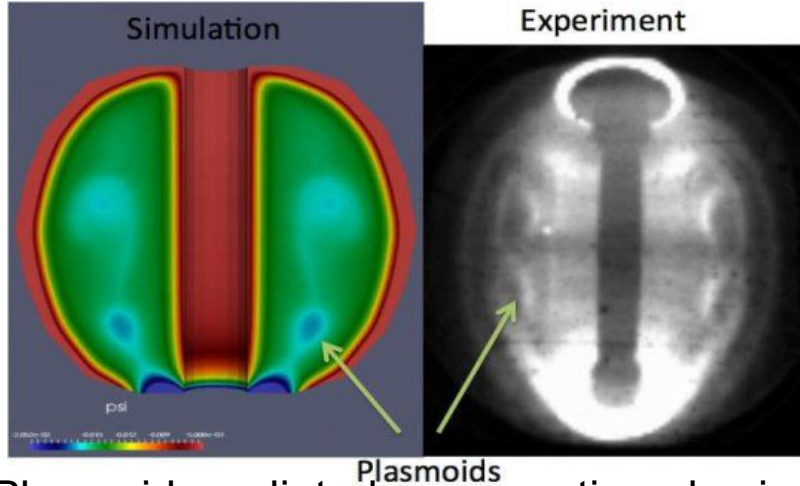


Burst-like phenomena in the core region of tokamaks.



Filamentary ELM structures in (a) NSTX (b) MAST (c) PEGASUS and (d) DIII-D

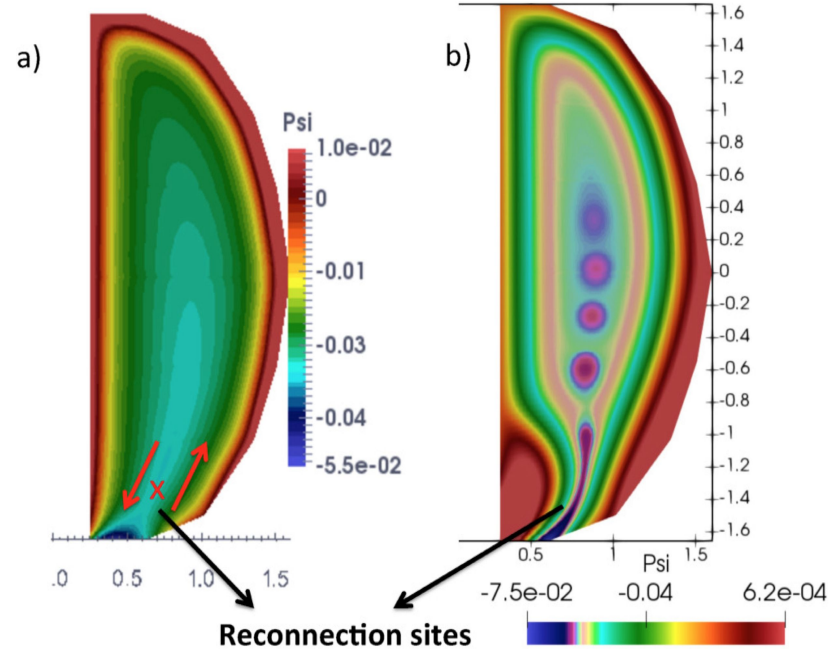
Fast magnetic reconnection has also been demonstrated in spherical tokamaks



Plasmoid-mediated reconnection physics, has been demonstrated during plasma start-up in NSTX

Ebrahimi&Raman PRL 2015

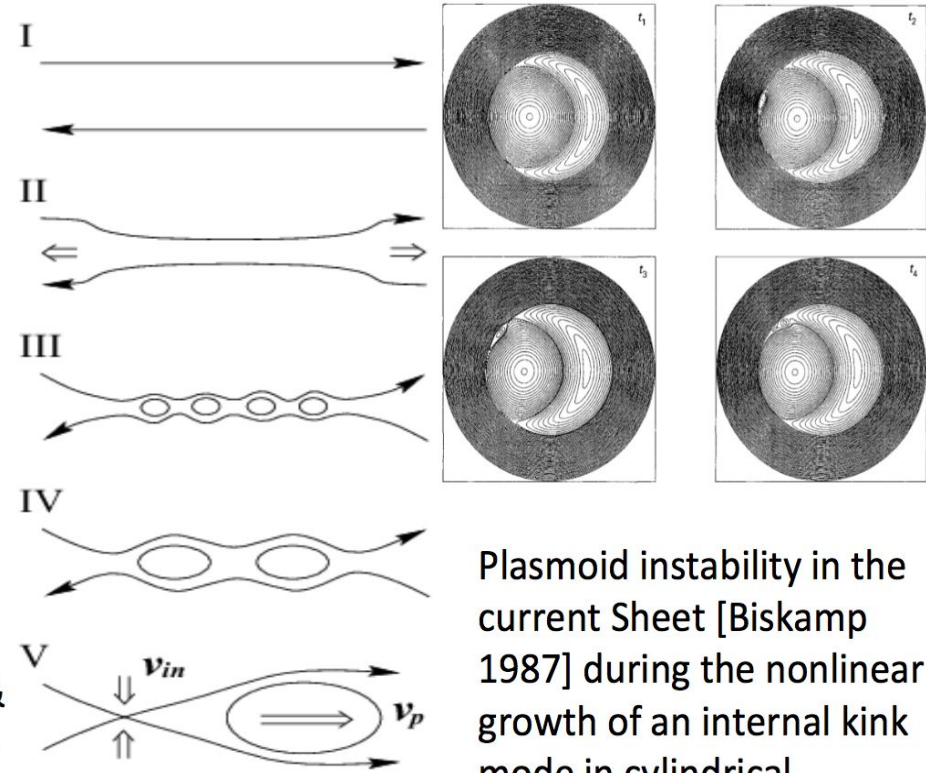
- For maximum plasma current formation fast reconnection is needed.



Also simulations in 3-D
Ebrahimi PoP 2019



- Elongated current sheet can become tearing unstable at high S . [Biskamp 1986, Tajima & Shibata 1997]
- Numerical and analytical development: [Shibata & Tanuma 2001, Loureiro et al. 2007; Lapenta 2008; Daughton et al. 2009,; Bhattacharjee et al. 2009, Cassak et al. (2009), Huang et al. 2011, 2013, Ebrahimi & Raman 2015, Uzdensky & Loureiro (2016)] **shows fast reconnection.**
- Static linear theory does not apply [Pucci & Velli (2014)] with a general theory [Comisso et al. PoP 2016]



Shibata & Tanuma 2001

Plasmoid instability in the current sheet [Biskamp 1987] during the nonlinear growth of an internal kink mode in cylindrical geometry [Gunter et al. 2015]



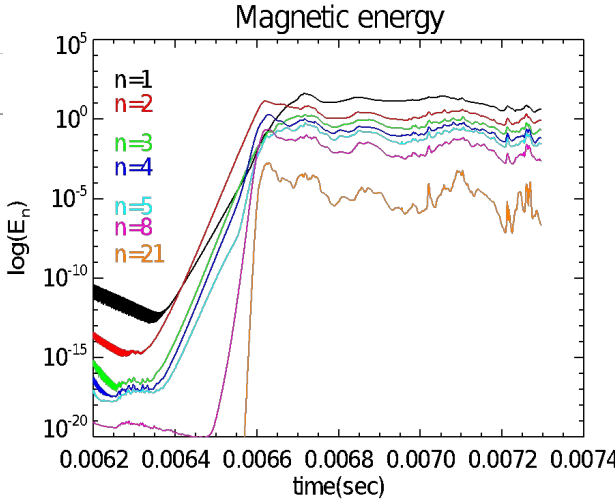
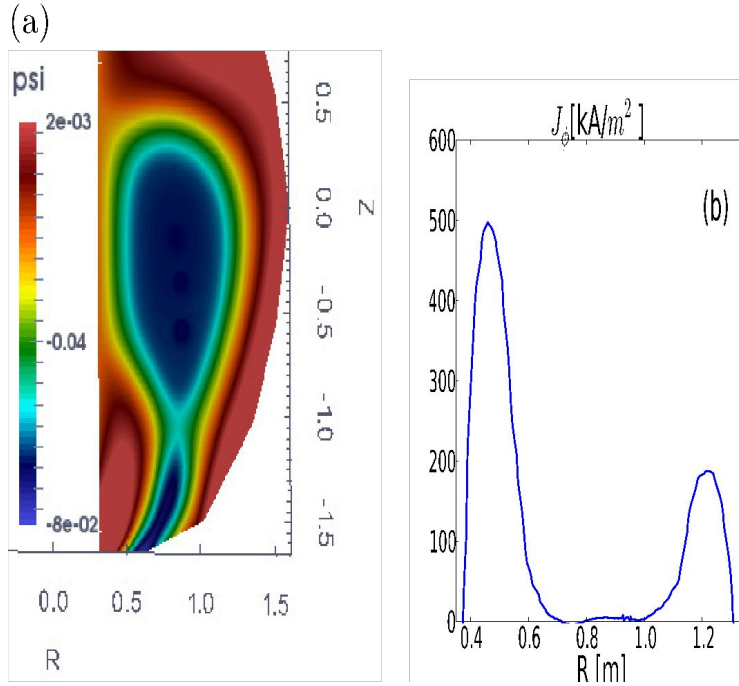
Edge current sheet/spikes can develop (Ebrahimi PoP 2017)

- during flux expansion
- from pressure-driven edge bootstrap current
- due to strong current ramp up
- during vertical displacement of plasma

Edge nonaxisymmetric current sheet instabilities grow on the poloidal Alfvén time scales and could cause

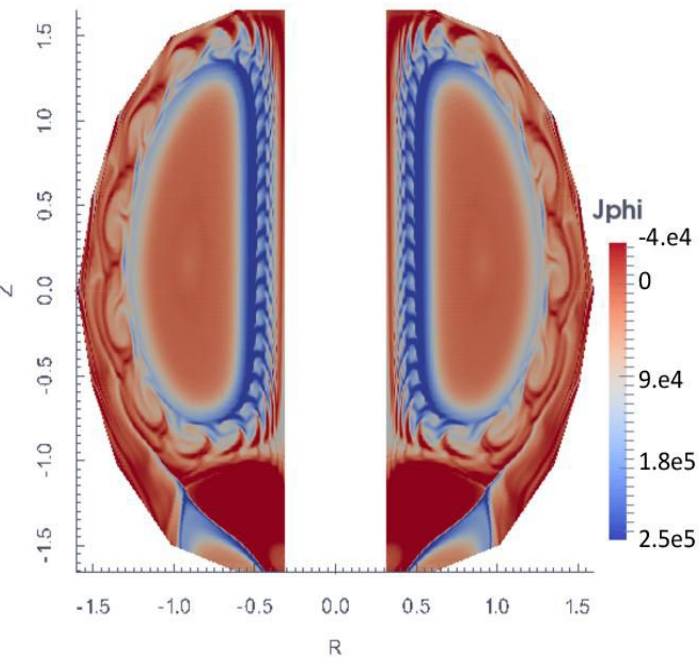
- I - poloidal flux amplification to trigger axisymmetric (2-D) reconnecting plasmoids formation
- II - low- n ELM peeling-driven filament structures
- III - reconnecting edge filaments during VDEs

3-D, non-axisymmetric magnetic fluctuations arise due to current-sheet instabilities localized near the edge region



- $J_\phi = 500\text{kA/m}^2$,
 $B = 0.7\text{T}$, $B_z = 0.1$
- higher toroidal modes numbers grow only nonlinearly and saturate at much lower amplitudes

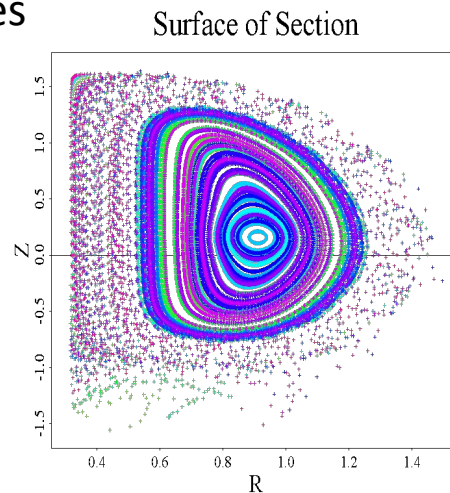
- n=1-6 linearly unstable,
- Edge modes grow on the poloidal Alfvén time scales



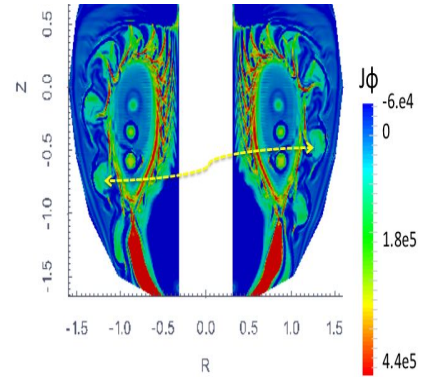
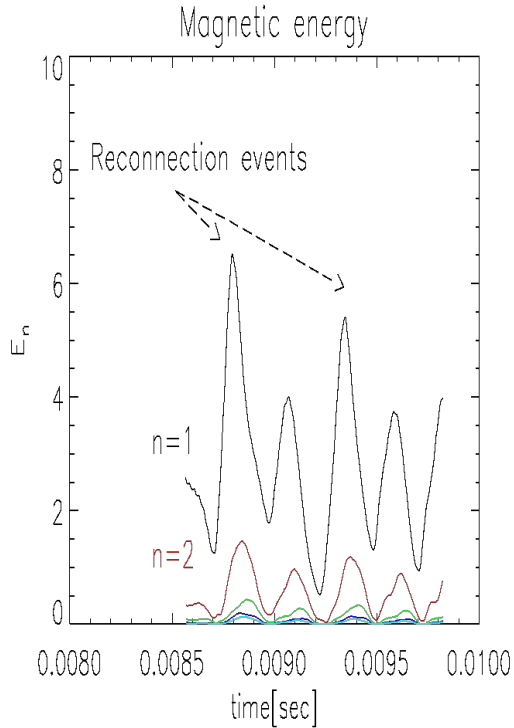
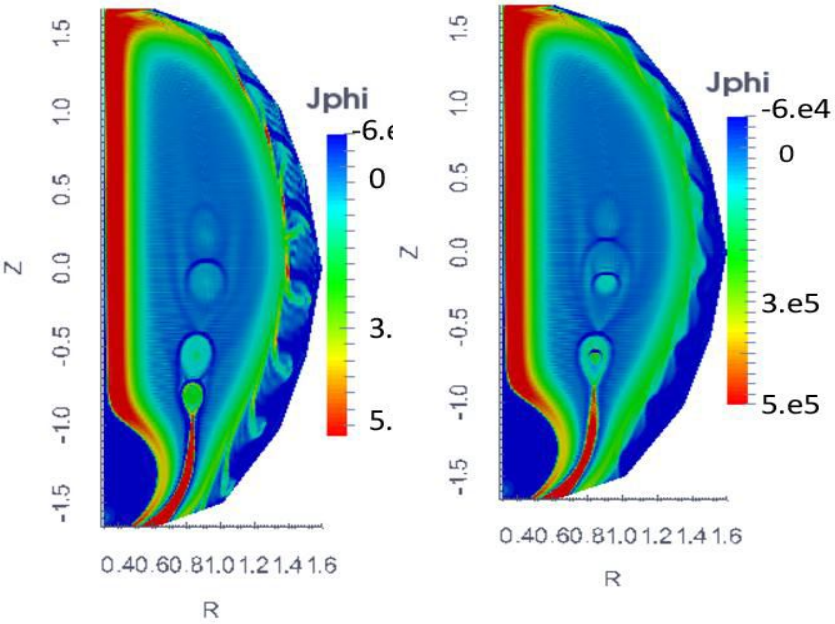
Ebrahimi PoP 2017

This model has been used to isolate nonlinear evolution of edge current from the core to study **onset and relaxation of SOL currents.**

- The onset of nonaxisymmetric edge current-sheet instabilities causes the formation of current-carrying filament structures radially extending from the closed flux region to the region of open field lines (outside of separatrix)
- Stochastic region outside of separatrix



Observed edge localized coherent structures exhibit repetitive cycles during nonlinear stage



The structures relax back radially to merge back into an axisymmetric toroidal current density



Averaging induction equation yields:

$$\frac{\partial \bar{\mathbf{B}}}{\partial t} = \nabla \times (\bar{\mathbf{V}} \times \bar{\mathbf{B}} + \bar{\mathcal{E}}_{emf} - \eta \nabla \times \bar{\mathbf{B}})$$

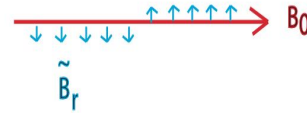
where

$$\bar{\mathcal{E}}_{emf} \approx \langle \tilde{\mathbf{V}} \times \tilde{\mathbf{B}} \rangle$$

is the mean EMF.

Terms only proportional to $\tilde{\mathbf{V}}$ and $\tilde{\mathbf{B}}$ (and the mean) would not contribute to the **mean** induction equation (due to Reynolds rule).

Consider:

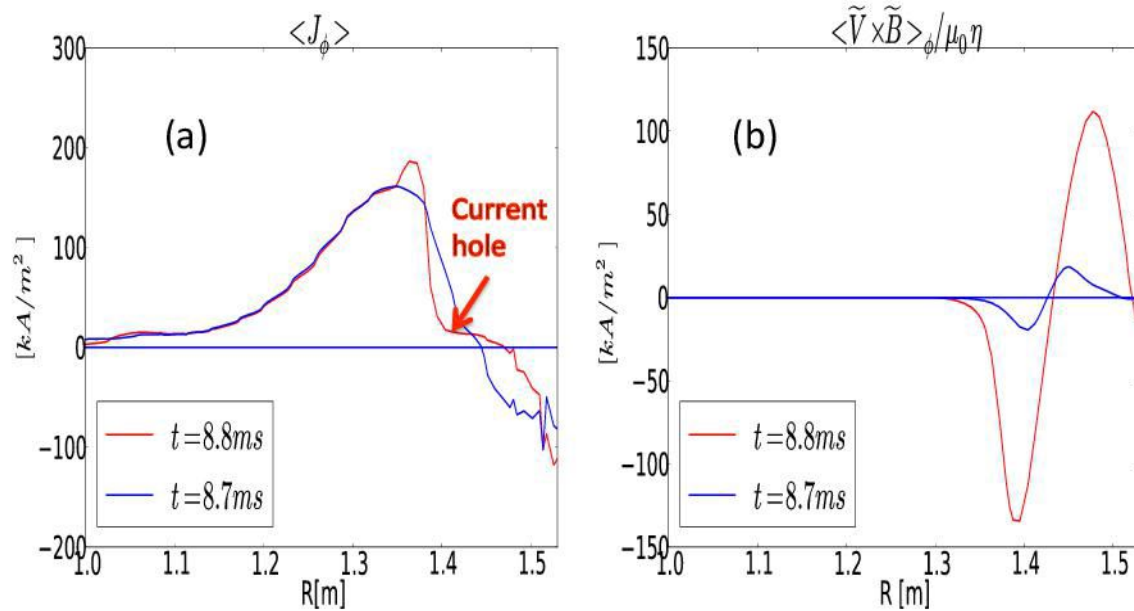


$$V = \langle V \rangle + \tilde{V}$$

$$B = \langle B \rangle + \tilde{B}$$

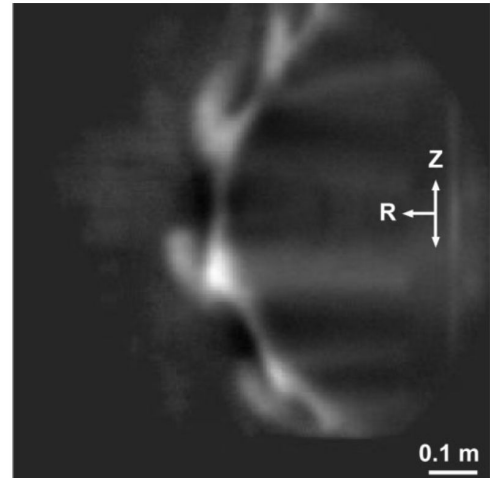
↑
↑
large-scale
small-scale

- fluctuations : $\tilde{\mathbf{B}}_{mn}(\mathbf{r}) = \tilde{\mathbf{B}}_{mn}(r)e^{i(m\phi - nz + \delta)} + \text{c.c}$
- $\langle \rangle$, or overbars \rightarrow **azimuthally and axially averaged - surface-averaged** $\int d\phi dz$
- Reynolds Rules $\implies \langle \tilde{\mathbf{B}} \rangle = \langle \tilde{\mathbf{V}} \rangle = 0$
Fluctuations can be instabilities.



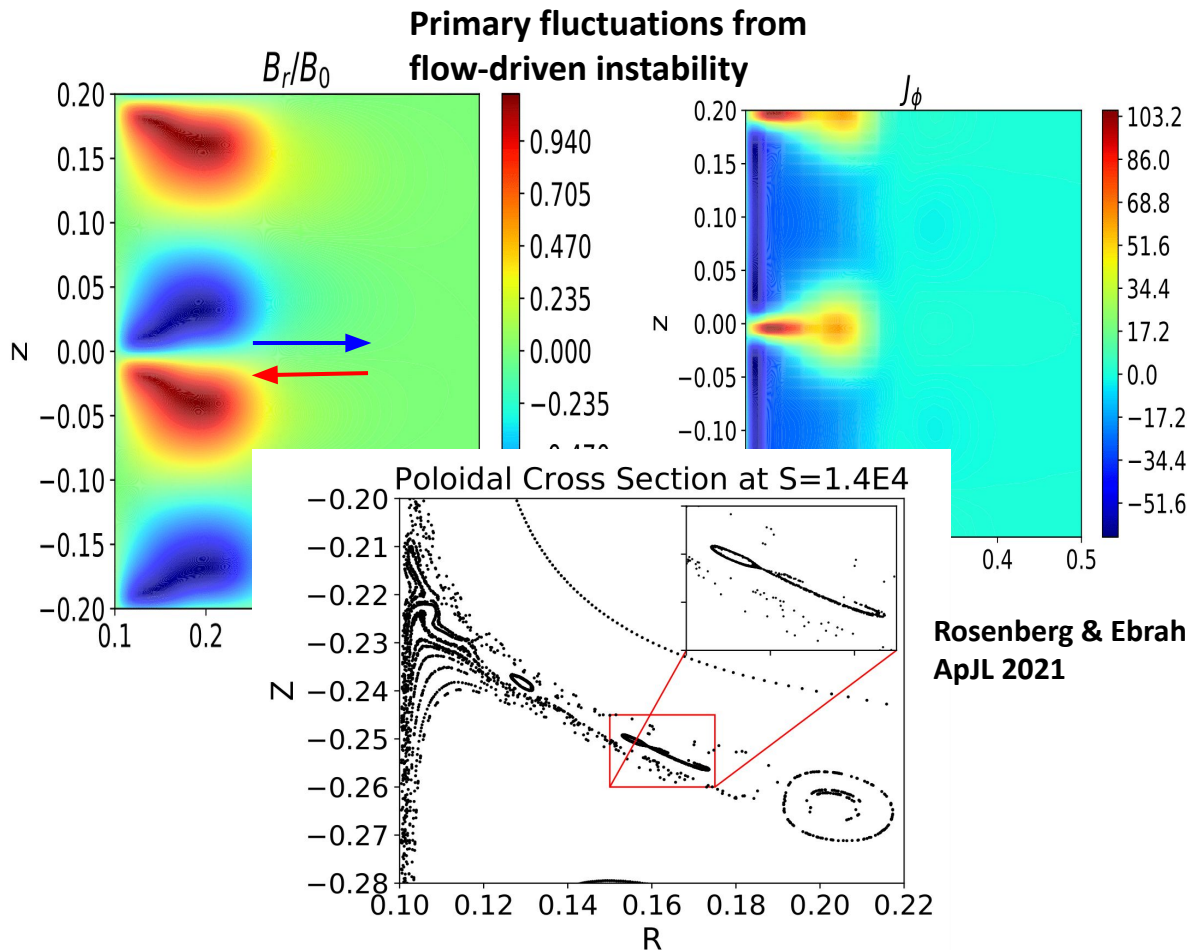
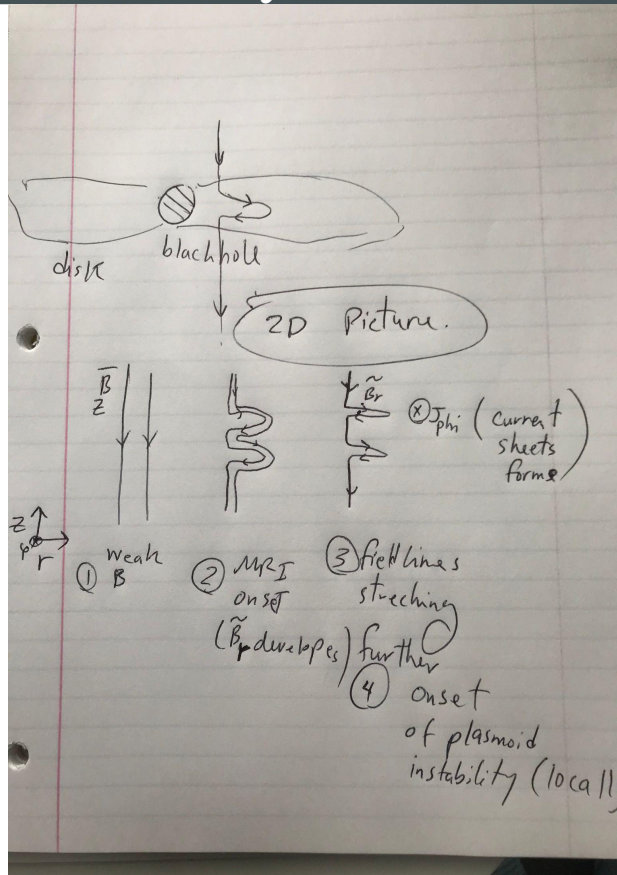
Coherent filament structures found here are very similar to the camera images of peeling modes from Pegasus

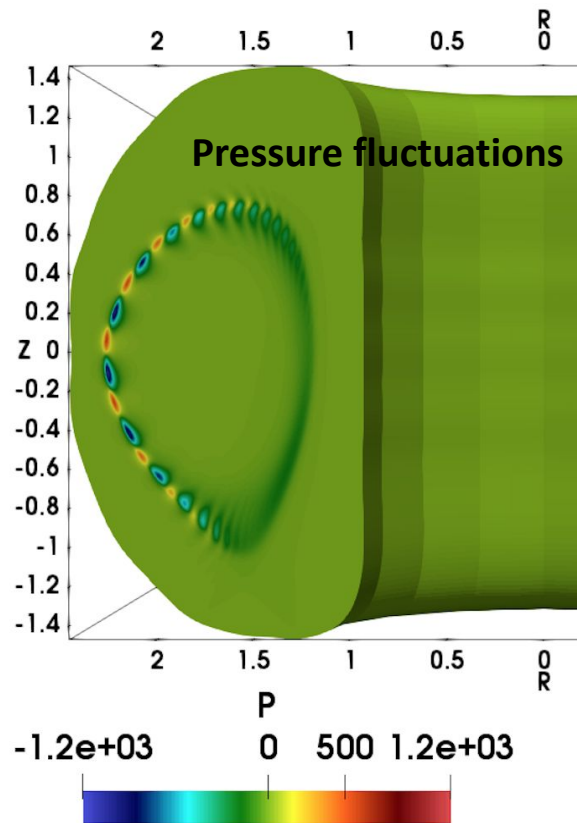
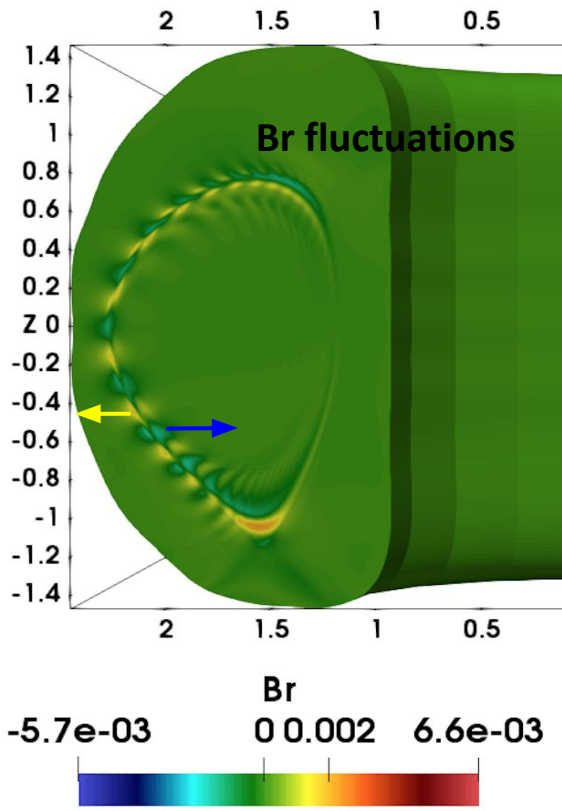
[Bongard, et al. PRL 2011, Thome et al. PRL 2016]



The localized dynamo term changes sign around the same radius where the flattening and annihilation of current density occurs [Ebrahimi PoP 2017]

How about current sheet formation due to a primary instability?





- As edge plasma interchangeably is displaced by the ballooning modes, local edge current sheet could form.



- Solves the linear and nonlinear MHD equations

$$\frac{\partial \mathbf{B}}{\partial t} = -\nabla \times \mathbf{E} + \kappa_{divb} \nabla \nabla \cdot \mathbf{B}$$

$$\mathbf{E} = -\mathbf{V} \times \mathbf{B} + \eta \mathbf{J} + \frac{1}{ne} \mathbf{J} \times \mathbf{B}$$

$$\mathbf{J} = \nabla \times \mathbf{B}$$

$$\frac{\partial n}{\partial t} + \nabla \cdot (n\mathbf{V}) = \nabla \cdot D \nabla n$$

$$\rho \left(\frac{\partial \mathbf{V}}{\partial t} + \mathbf{V} \cdot \nabla \mathbf{V} \right) = \mathbf{J} \times \mathbf{B} - \nabla P - \nabla \cdot \Pi$$

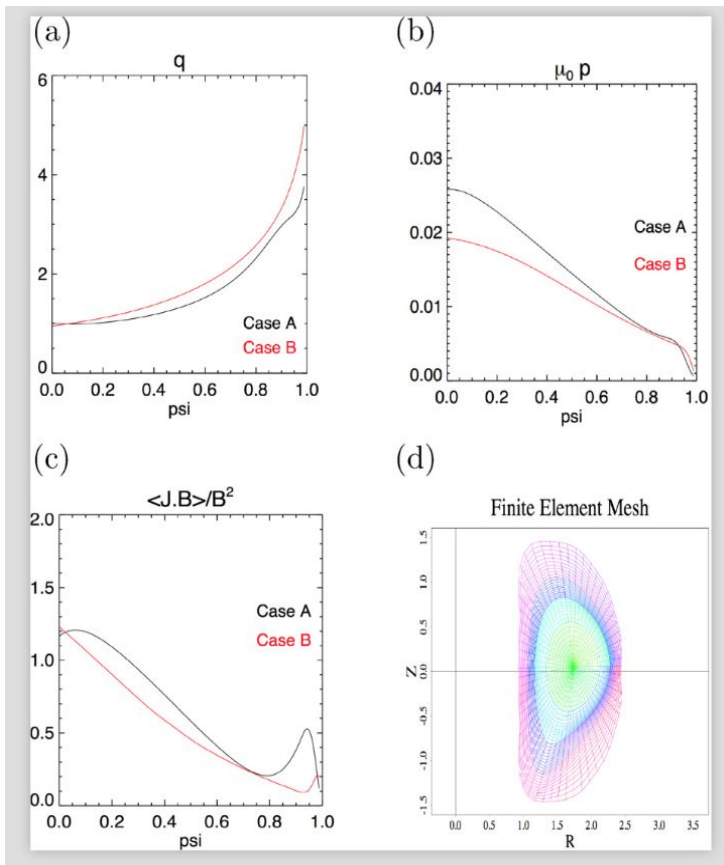
$$\frac{n}{(\Gamma - 1)} \left(\frac{\partial T_\alpha}{\partial t} + \mathbf{V} \cdot \nabla T_\alpha \right) = -\rho_\alpha \nabla \cdot \mathbf{V} - \nabla \cdot \mathbf{q}_\alpha + Q$$

- $\mathbf{q} = -n[(\kappa_{||} - \kappa_{\perp})\hat{b}\hat{b} + \kappa_{\perp}\mathbf{I}] \cdot \nabla T$

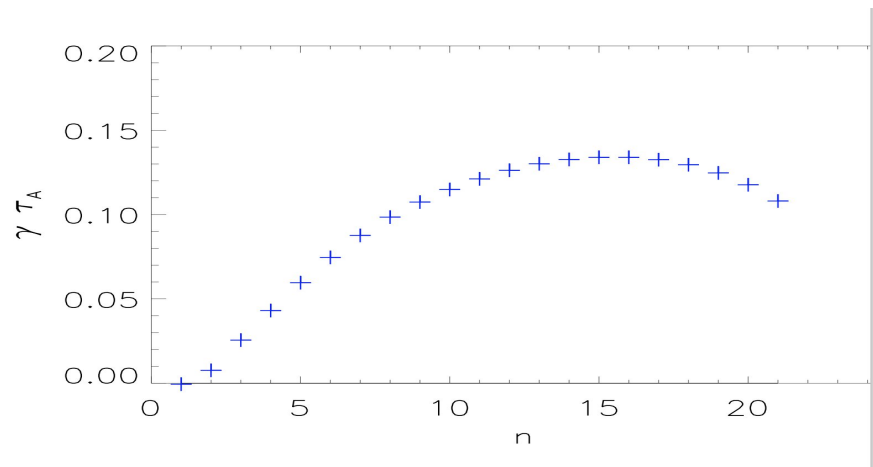
- Π is the stress tensor (also includes numerical $\rho\nu\nabla V$)

I. Reconnection studies in Peeling-Ballooning DIII-D plasmas

- The spatial resolution is 40x60 fifth or sixth order polynomials in the poloidal plane, and 86 toroidal modes are used. With an anisotropic pressure model (perpendicular and parallel thermal diffusivities of 25 and 2e6)
- Use either temperature-dependent Spitzer or constant magnetic diffusivity.
- G. Dong (X. Liao et al. PoP 2016) and D. Brennan (et al. J. physics 2006) for providing two DIII-D eqdsk files



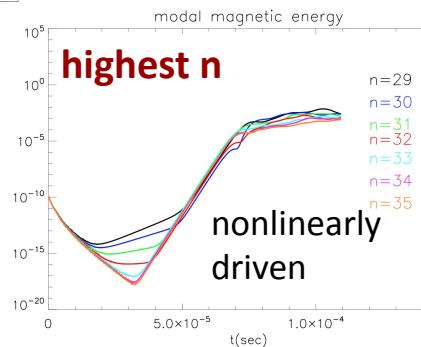
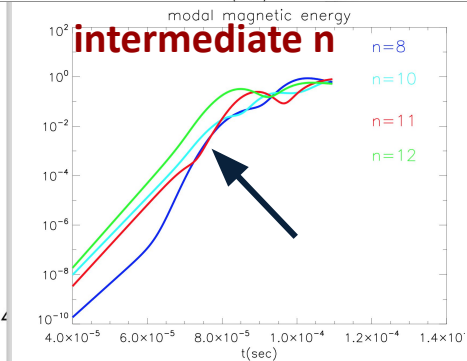
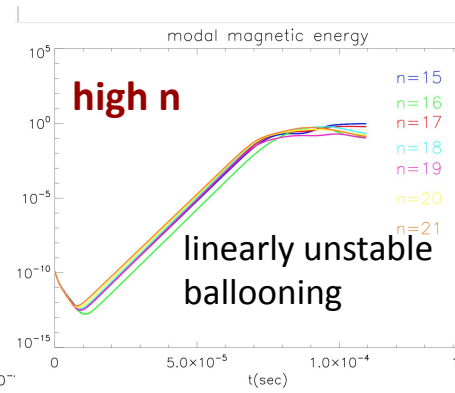
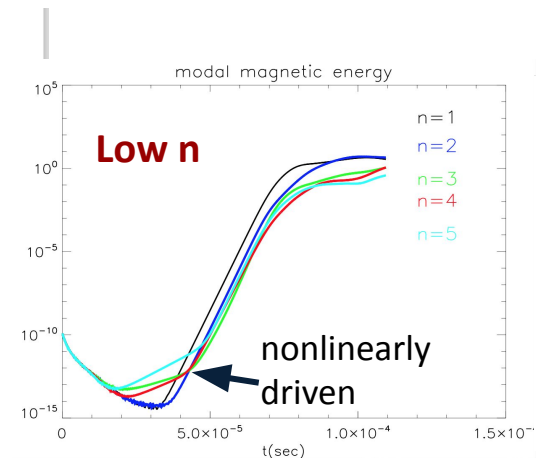
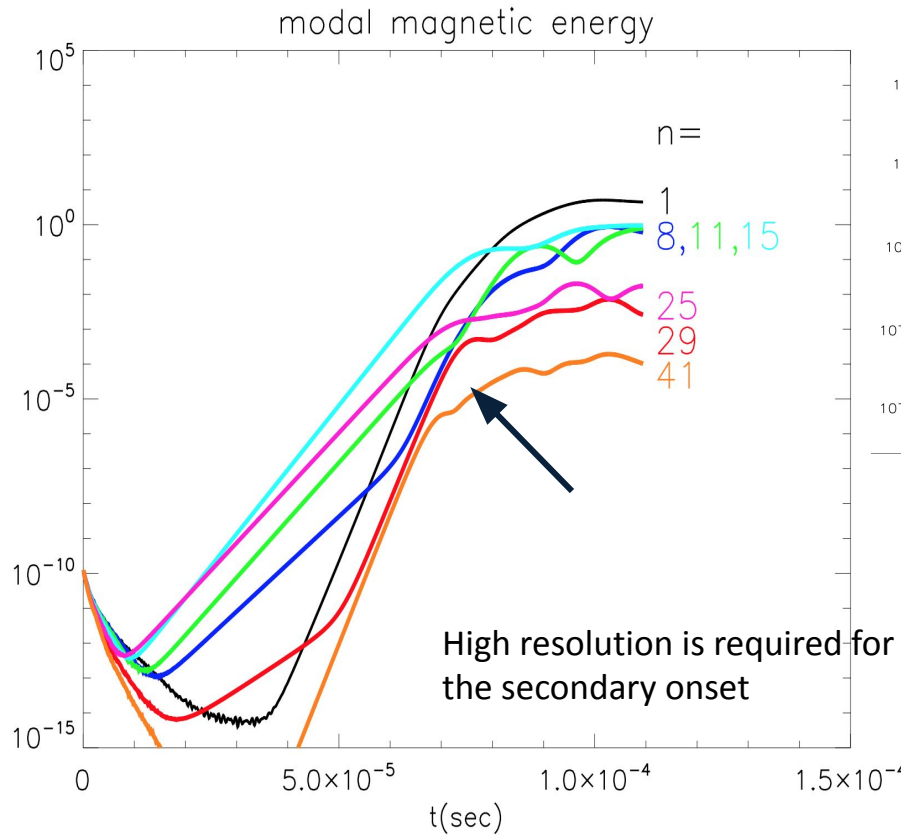
NIMROD simulations are performed starting with equilibrium profiles from DIII-D 145701 discharge.

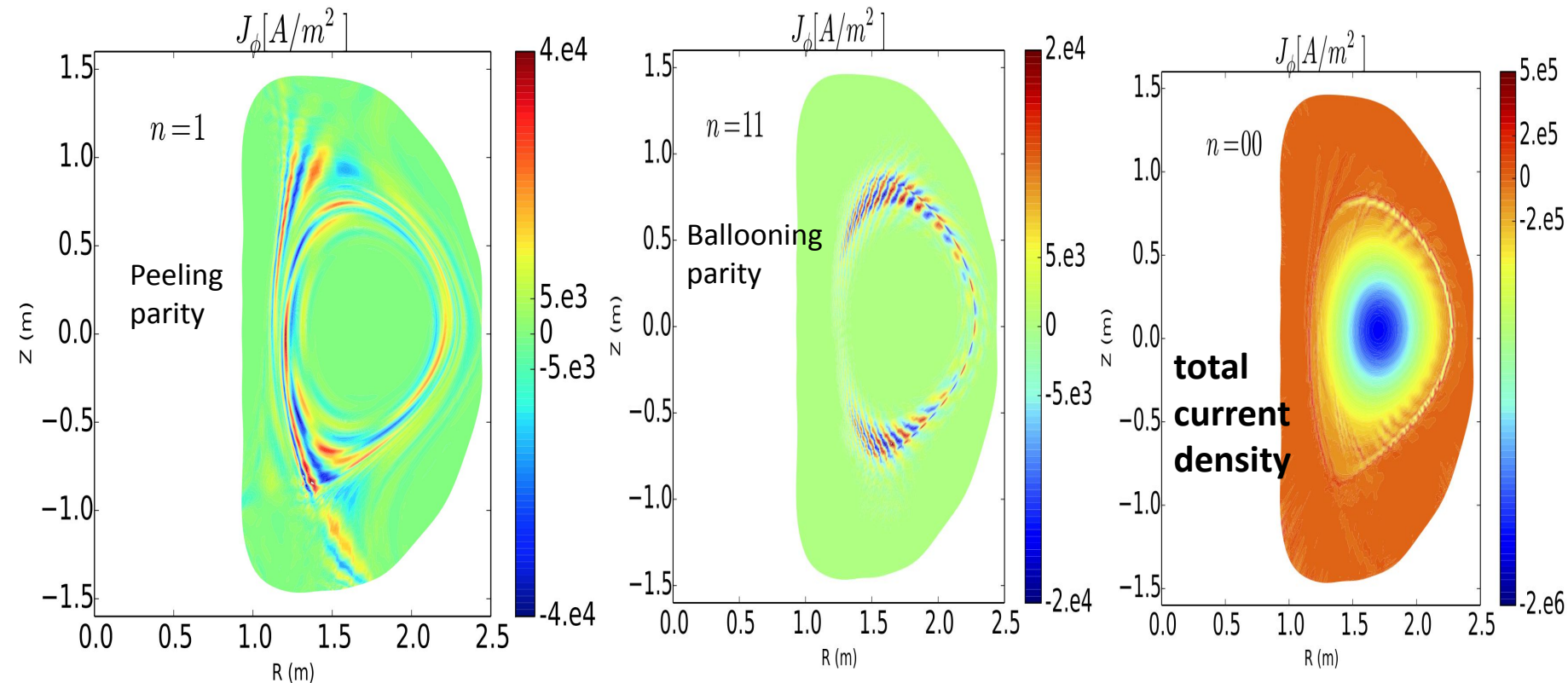


- Low n modes are linearly stable.

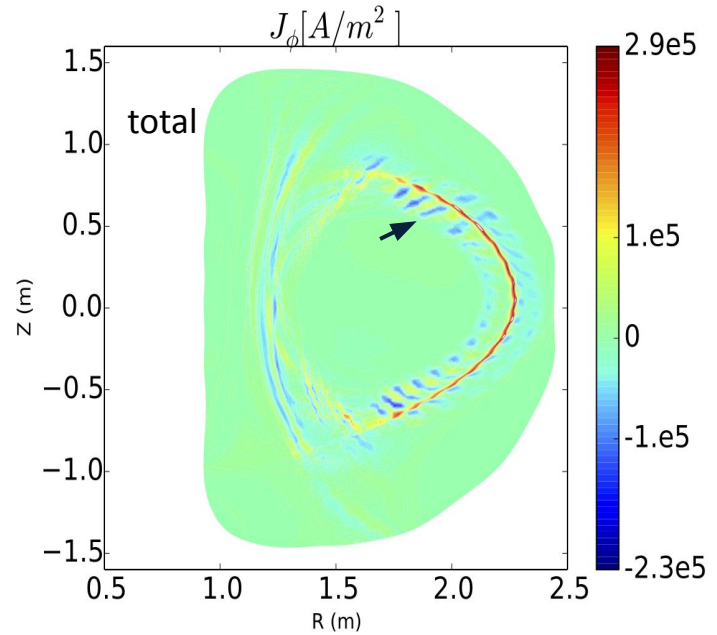
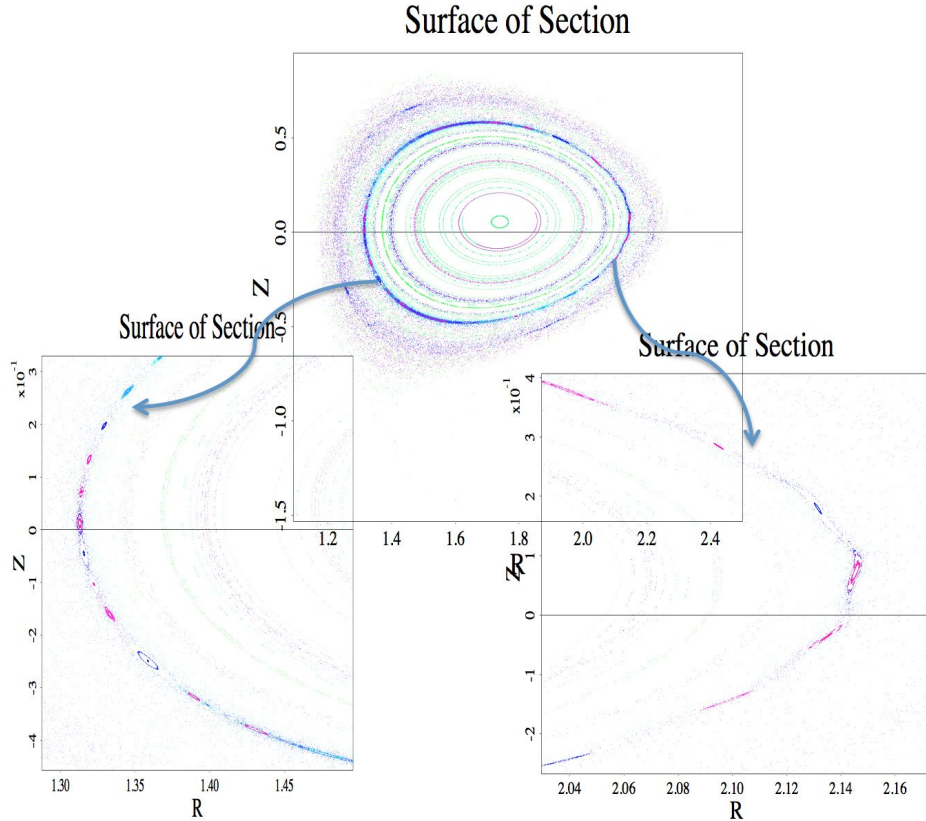
Ebrahimi submitted 2021

Low- n grow nonlinearly while intermediate n ballooning modes exhibit secondary faster exponential growth



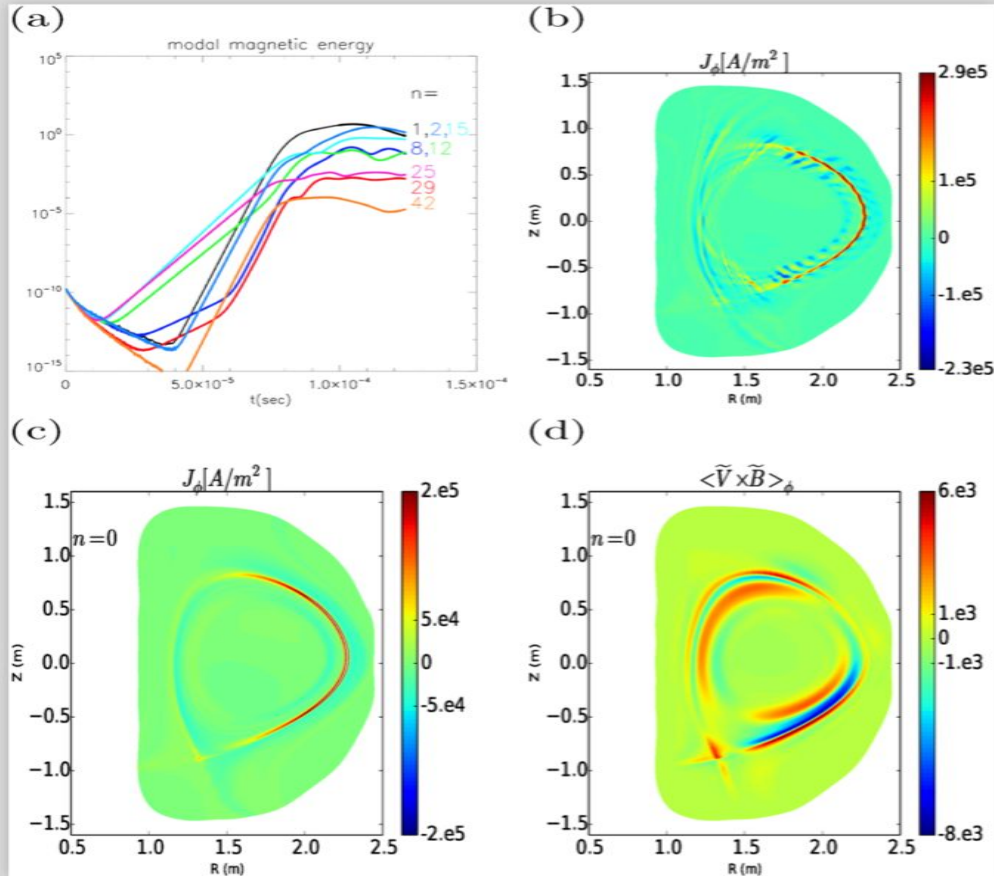


Magnetic islands are co-located with the current density finger structures.



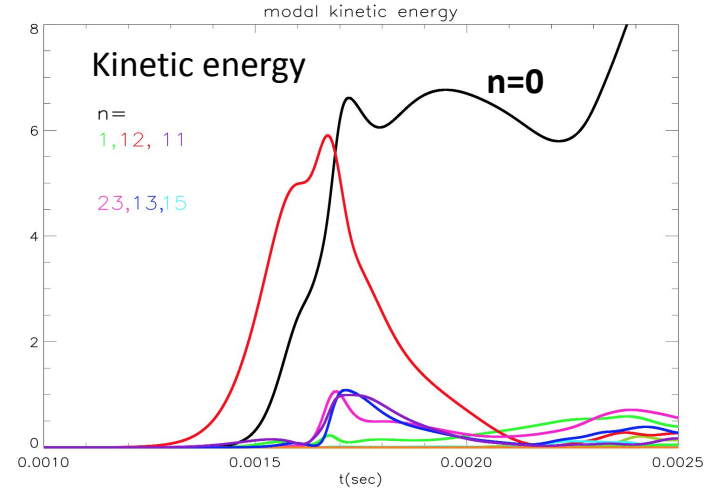
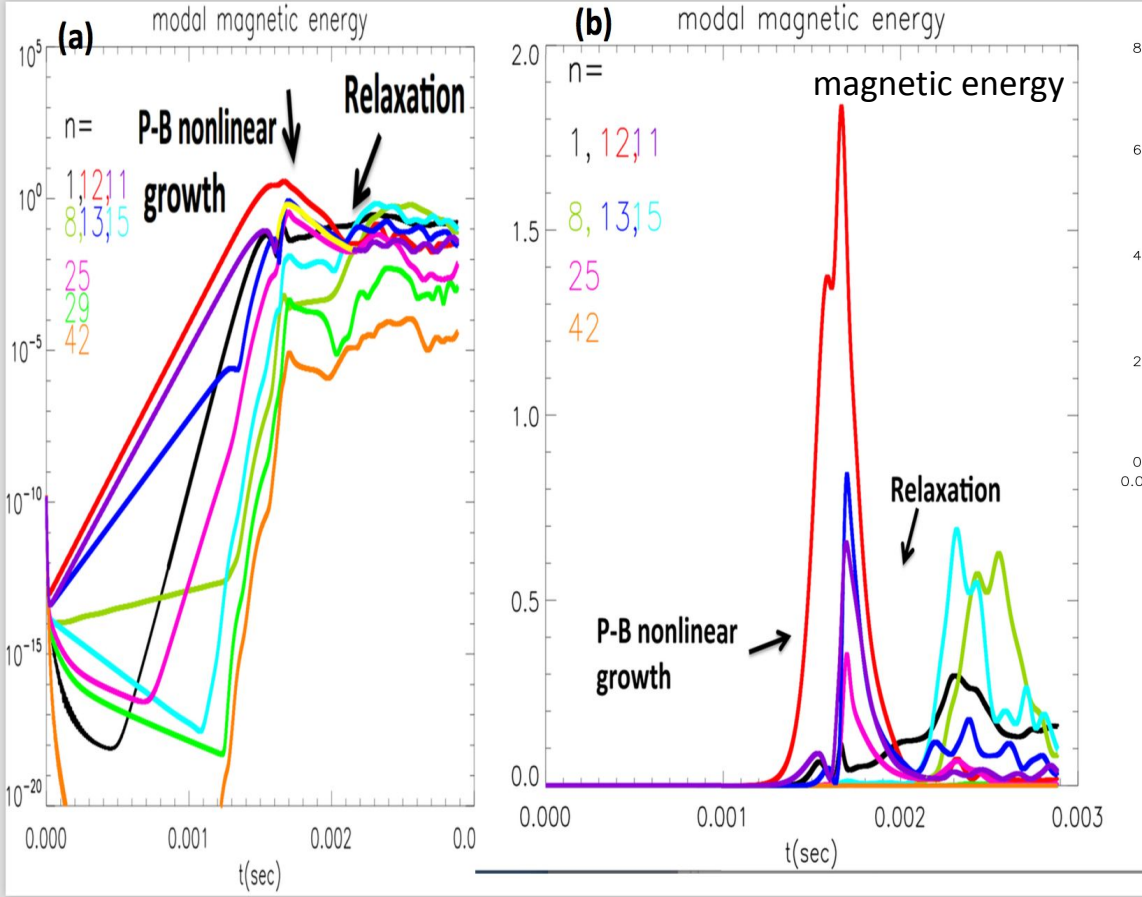
Stochastic regions due to nonlinear overlapping of several high-n

Linearly stable low- n peeling modes grow nonlinearly and saturate at large amplitudes.



- Two types of current sheets of poloidally extending (R,Z) (type 1) and radially extending blobs of current (type 2) are generated as the modes saturate.
- The axisymmetric current density is nonlinearly generated by the P-B modes to suppress source of instability itself.
- Toroidally averaged emf exhibits a bi-directional structure, which is consistent with formation of axisymmetric toroidal current density.

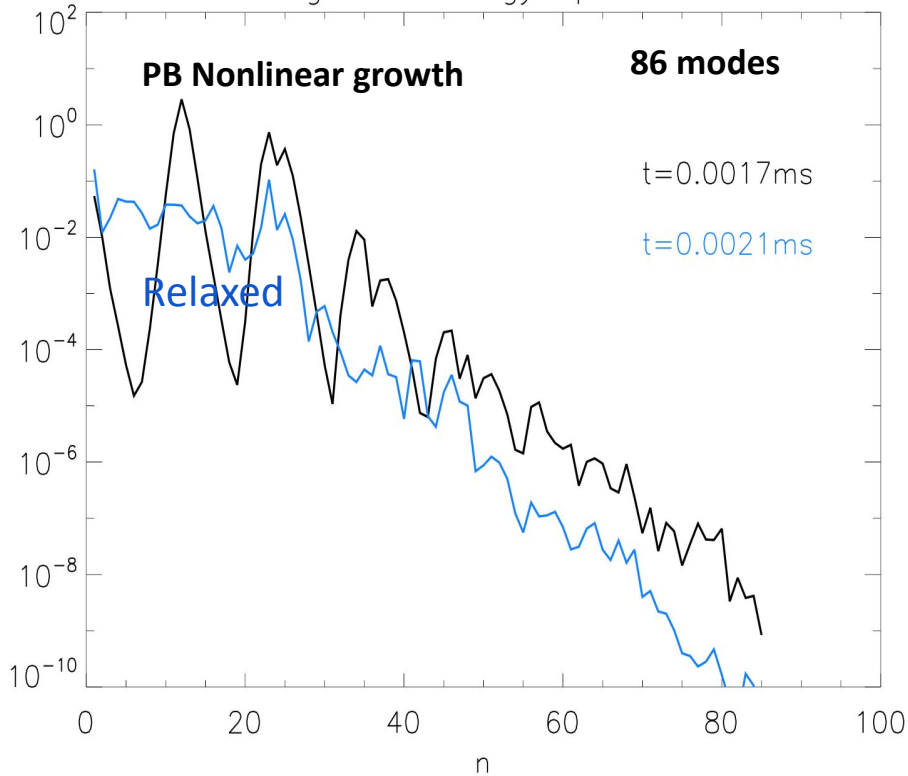
Self-consistent ELM calculations show that plasma edge goes through magnetic self-organization.



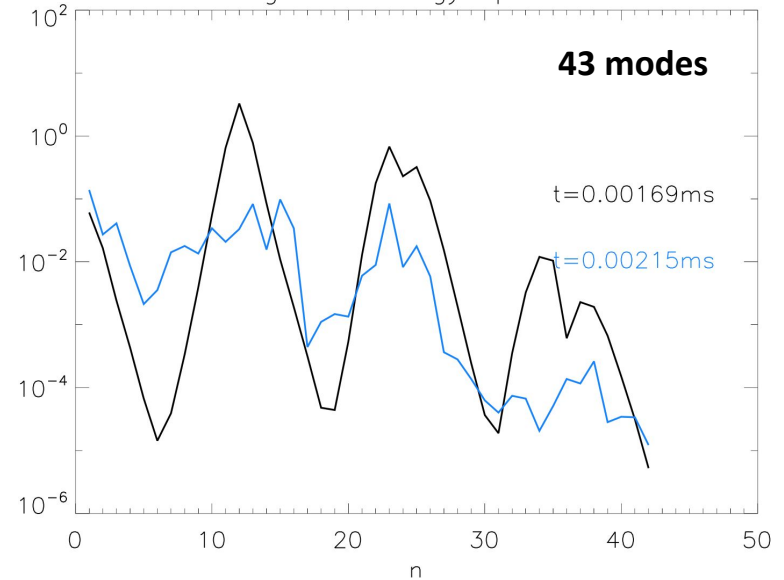
- Linearly unstable intermediate-n ballooning modes and the nonlinearly driven peeling-type low-n modes grow and saturate.
- During the reconnection burst kinetic energy is enhanced



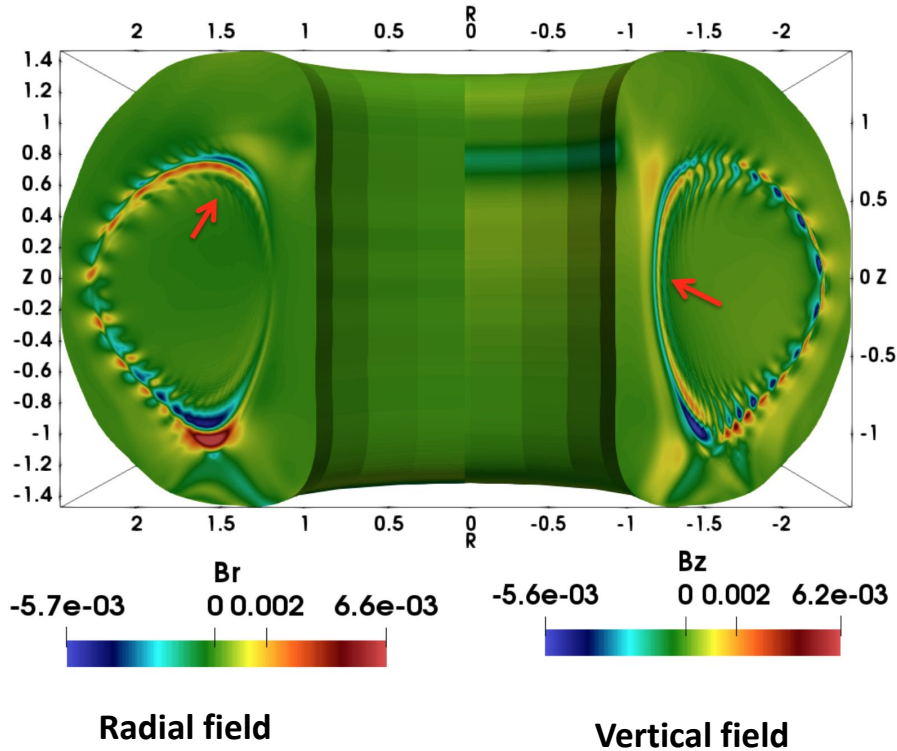
magnetic energy spectrum



magnetic energy spectrum



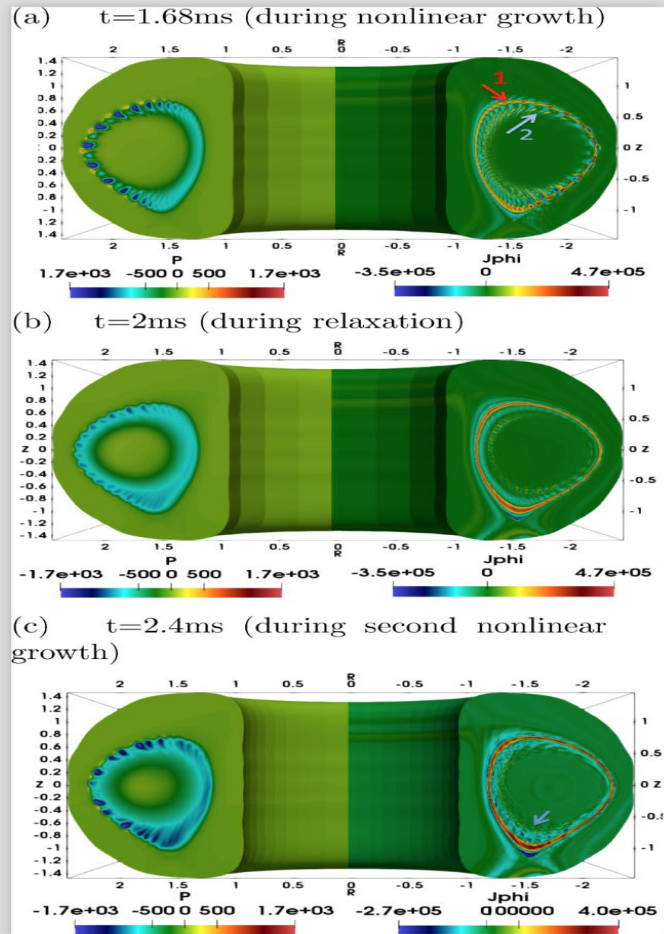
Almost identical results with half the number of toroidal modes.



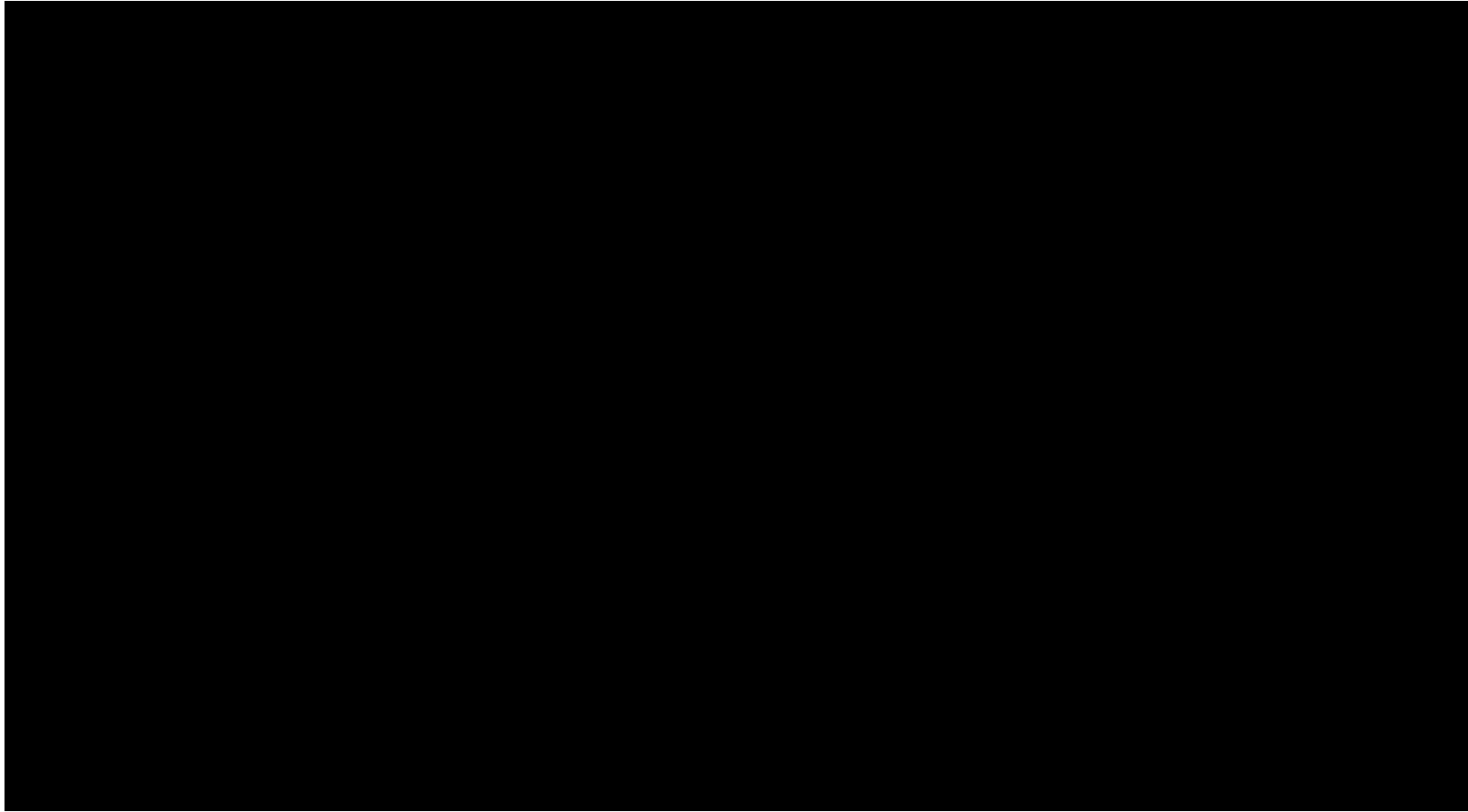
- The vertical variation of the generated radial zonal magnetic (shown by red arrow on the left side), combined with the radial variation of vertical magnetic (red arrow on the right side of), produces an axisymmetric ($n=0$) toroidal current density.

$$\mu_0 J_\phi = \frac{\partial B_r}{\partial z} - \frac{\partial B_z}{\partial r}$$

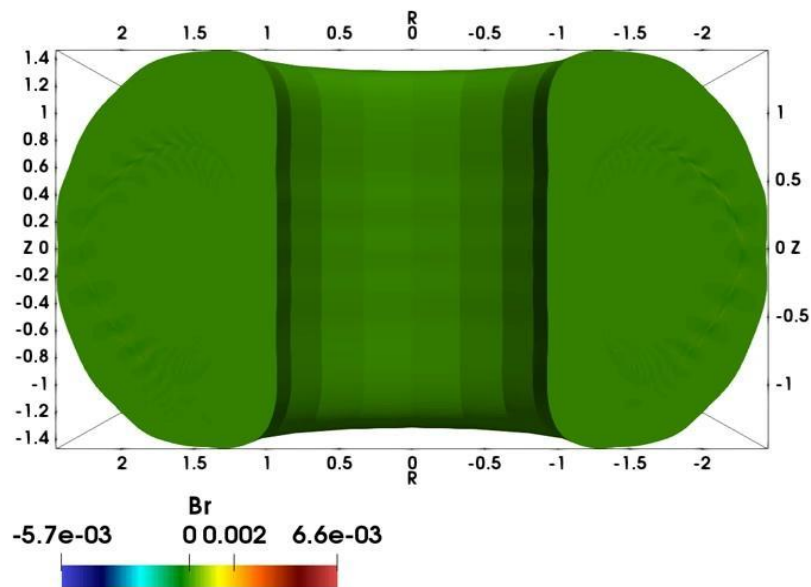
- Radial (and poloidal) current expulsion occurs in the form of 3D plasmoids in the region of the SOL during a bursty reconnection process (a sudden growth followed by relaxation).



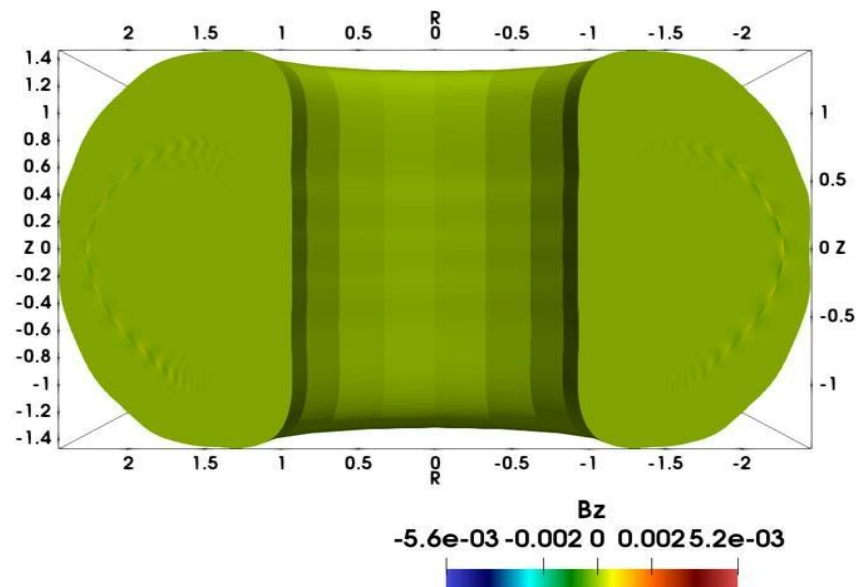
- Two types of current sheets are identified during the nonlinear evolution. The first one is the poloidally extended axisymmetric current sheet (shown by arrow 1).
- The second type of current sheet is the finger-type non-axisymmetric current sheets radially and vertically extending inside and out of the SOL (shown by the arrow numbered 2). These latter current sheets further break and leave small-scale current blobs (plasmoids) as the modes nonlinearly saturate.

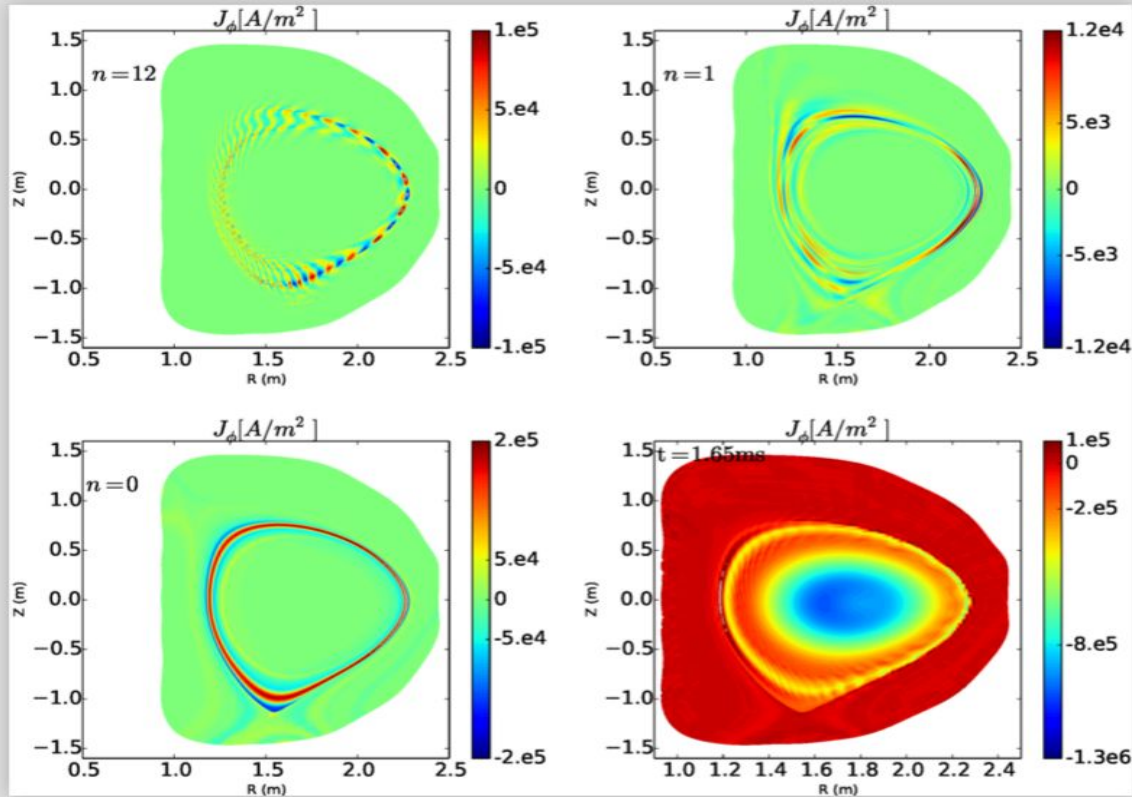


Time: 0.00125

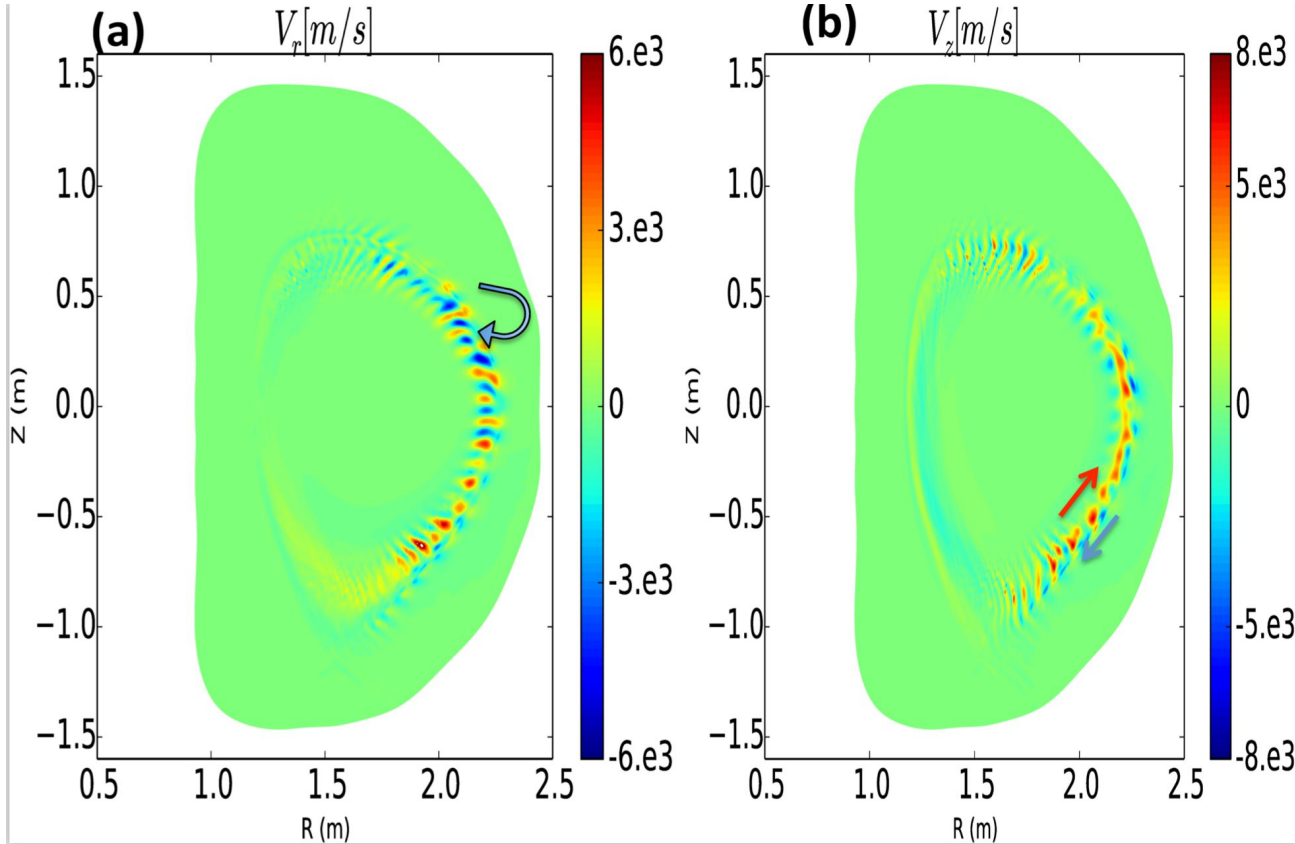


Time: 0.00125



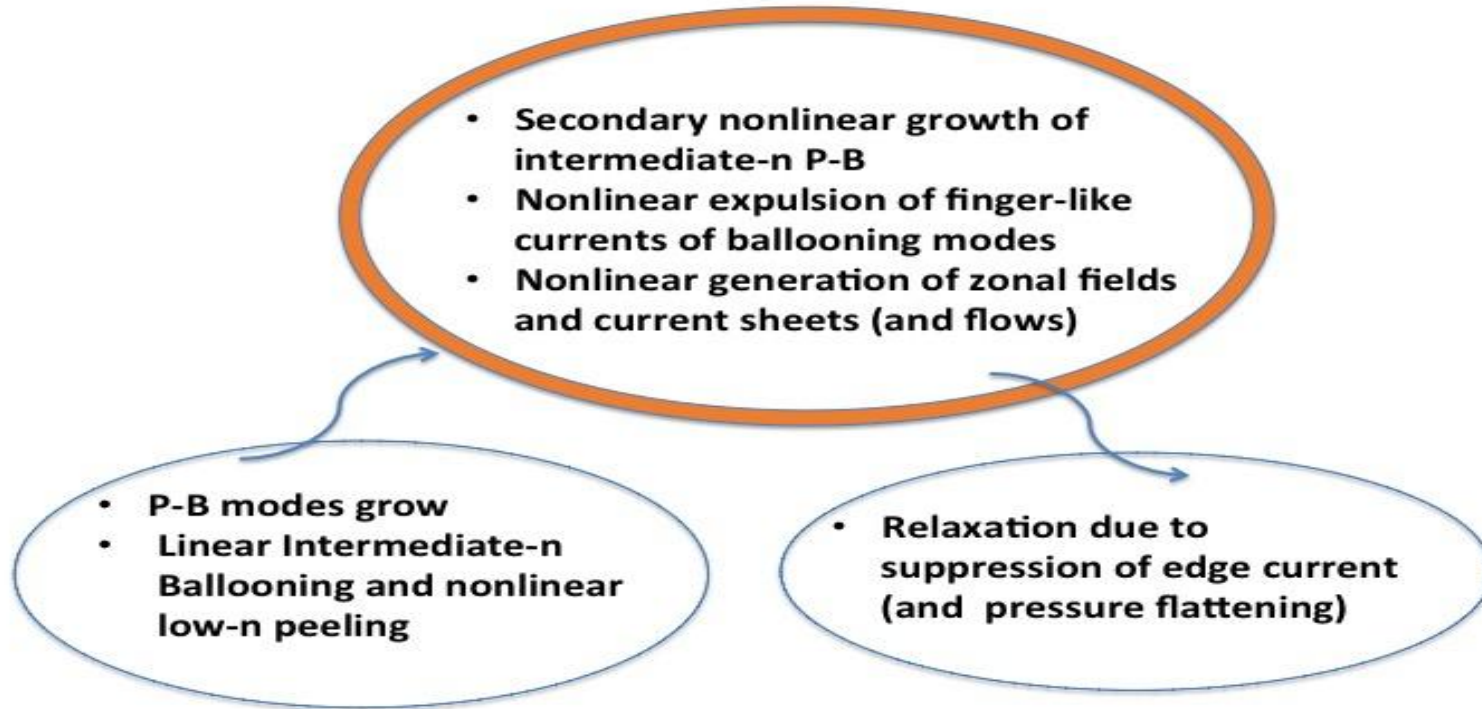


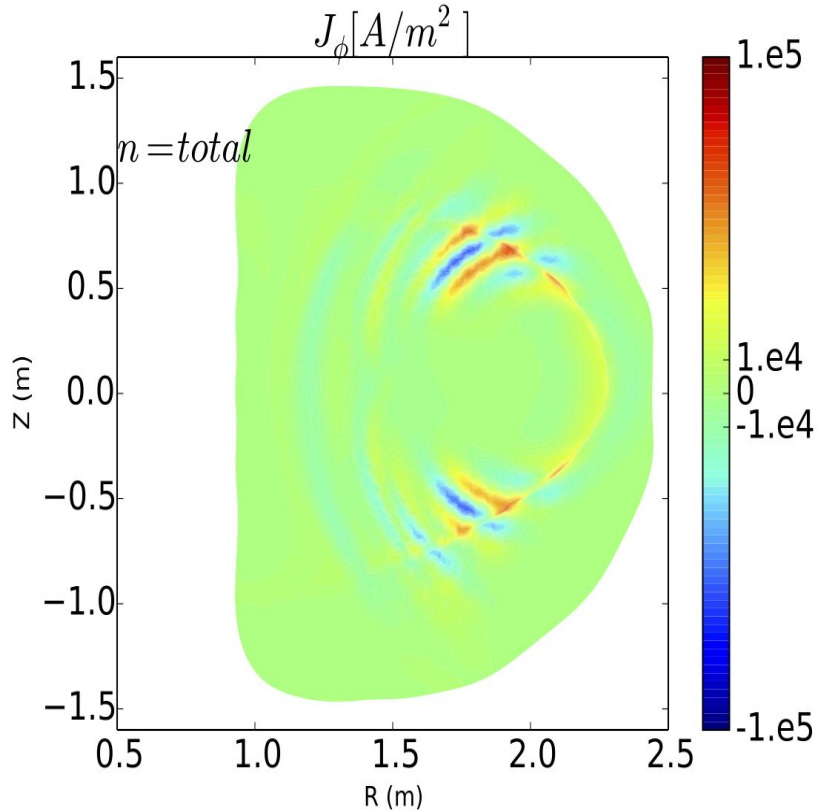
- Modal decomposition of peeling and ballooning components of ELMs, also show the nonlinearly generation of axisymmetric current sheets that suppress edge peeling drive and lead to relaxation of ELMs.





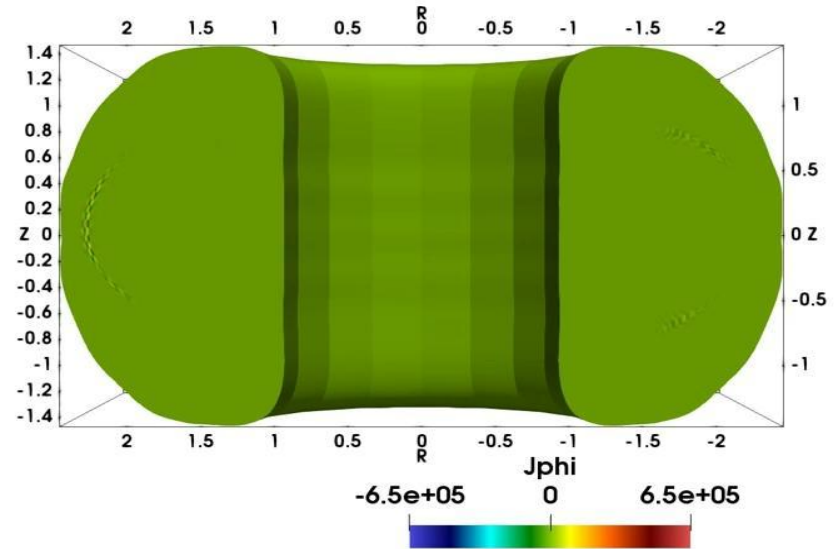
- Edge current-sheet instabilities cause the formation of radially extending current-carrying plasmoids
- Through novel 3D simulations, it is shown that filaments emerging from nonlinear ballooning instabilities display strong current sheets leading to the formation of plasmoids and bursty reconnection dynamics.
- It is during a secondary sudden nonlinear growth of P-B modes that nonlinear finger-like structures of ballooning modes are expelled into the outer edge region.
- It is uncovered that nonlinearly generated axisymmetric current sheets suppress edge peeling drive and lead to relaxation of ELMs





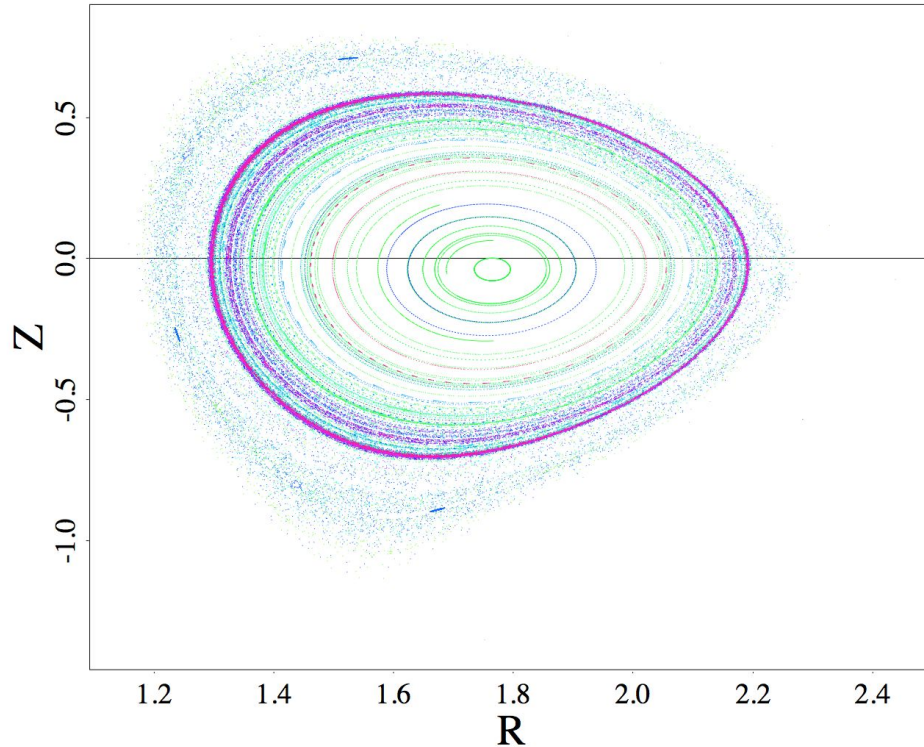
S~103

Time: 6.7329e-05

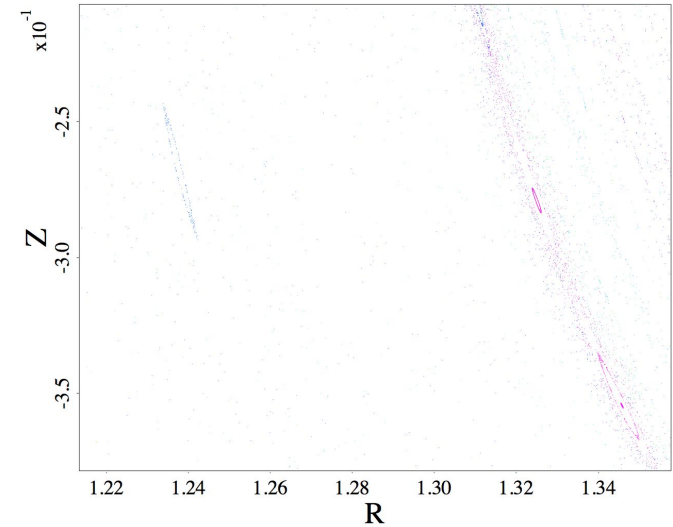


S~105

Surface of Section



Surface of Section



Case A at fixed magnetic diffusivity